

## THE EFFECT OF ATMOSPHERIC COLD PLASMA CLEANING OF FTO SUBSTRATES ON THE QUALITY OF TiO<sub>2</sub> ELECTRON TRANSPORT LAYERS FOR PRINTED CARBON-BASED PEROVSKITE SOLAR CELLS

<sup>1</sup>Matej HVOJNIK, <sup>2</sup>Július VIDA, <sup>2</sup>Tomáš HOMOLA, <sup>1</sup>Michaela PAVLIČKOVÁ, <sup>1</sup>Michal HATALA, <sup>1</sup>Milan MIKULA, <sup>1</sup>Katarína TOMANOVÁ, <sup>1</sup>Pavol GEMEINER

<sup>1</sup>Faculty of Chemical and Food Technology, Slovak University of Technology in Bratislava, Slovakia, EU, [matej.hvojnisk@stuba.sk](mailto:matej.hvojnisk@stuba.sk)

<sup>2</sup>Department of Physical Electronics, Faculty of Science, Masaryk University, Brno, Czech Republic, EU

<https://doi.org/10.37904/nanocon.2020.3716>

### Abstract

In this work, TiO<sub>2</sub> electron transport layers (ETL) of printed perovskite solar cells with back carbon electrode (C-PSCs) were prepared on uncleaned, chemically cleaned, and plasma-treated FTO substrates. The effect of cleaning procedure type on the quality of TiO<sub>2</sub> ETL has been characterised by XPS and SEM. The C-PSCs with FTO substrates treated by low-temperature atmospheric plasma at ambient air for 10 s reached approximately the same efficiency (4.4%) as with the chemically cleaned FTO (4.5%). From optical microscope and SEM images, it was observed that the plasma cleaned the FTO substrate to some extent, thereby reducing the number of defects and pinholes occurring in the blocking layer. XPS measurements confirmed that chemical and plasma treatment significantly reduced organic species on the FTO surface.

**Keywords:** Atmospheric cold plasma, TiO<sub>2</sub>, electron transport layer, carbon electrode, perovskite solar cells

### 1. INTRODUCTION

The role of the electron transport layer (ETL) of carbon-based perovskite solar cell (C-PSC) is to extract and transport electrons from the perovskite layer towards the transparent conductive oxide (TCO) electrode (glass or PET substrate with FTO or ITO layer). The quality of the ETL depends on two main parameters: 1) the preparation process and the composition of the used dispersion, which determine its thickness, roughness, and compactness; 2) the surface properties of the used substrate [1]. The most suitable ETL layer is very thin (<50 nm), which results in defects that cause internal short-circuits after the undesirable contact between the perovskite and TCO [2,3]. On the other hand, if the layer is too thick, the series resistance increases, the electrons recombine with the holes, resulting in a reduction of the current density and the fill factor of the solar cell [4,5]. The ETL with a thickness of several tens of nanometres is applied on the pre-treated substrates, and even the smallest impurity related to insufficient cleaning can significantly affect the quality of the ETL as well as the performance of the entire PSC. The most commonly used method of cleaning is chemical cleaning, which is very effective, but on the other hand, it is time-consuming (~1 hour) and requires the use of harmful organic solvents [6].

In this work, we showed that rapid (in order of seconds) atmospheric plasma treatment in ambient air has a potential to replace chemical cleaning of FTO substrates, and we examined the effect of plasma on FTO surface and the quality of TiO<sub>2</sub> ETL deposited on FTO. In addition to substrate cleaning, plasma also increases the surface energy and ensures better ETL homogeneity and charge transport at its interface with FTO.

## 2. EXPERIMENTAL SECTION

### 2.1. Materials

FTO/glass substrates (fluorine-doped tin oxide,  $7 \Omega/\text{sq.}$ ), titanium diisopropoxide bis(acetylacetonate) (75 wt.% TiAcAc in isopropanol), isopropyl alcohol ( $\geq 99,7\%$  ( $\text{CH}_3$ )<sub>2</sub>CHOH), diethanolamine ( $\geq 98$  wt.%, DEA) were purchased from Sigma-Aldrich. Titanium tetrachloride ( $\geq 97\%$ ,  $\text{TiCl}_4$ ) was ordered from Merck KGaA. Ethanol ( $\geq 97\%$ ,  $\text{CH}_3\text{CH}_2\text{OH}$ ) was from mikroCHEM. Mesoporous titania nanoparticle paste (Ti-Nanoxide T165/SP), mesoporous zirconium dioxide nanoparticle paste (Zr-Nanoxide ZT/SP), mesoporous carbon-black paste (Elcocarb B/SP) and perovskite solution ( $(5 - \text{AVA})_x(\text{MA})_{1-x}\text{PbI}_3$ ) were purchased from Solaronix.

### 2.2. Device fabrication

Printed mesoporous perovskite solar cells with carbon back electrode (C-PSCs) were prepared on the commercial FTO/glass substrates cleaned by three different methods: chemically cleaned, plasma-treated, and uncleaned. The preparation process of solar cells with the structure (**Figure 1**): FTO glass substrate/electron transport – blocking layer  $\text{TiO}_2$ /mesoporous  $\text{TiO}_2$  layer/scaffold  $\text{ZrO}_2$  layer/carbon back electrode/perovskite ran under laboratory conditions. The chemical cleaning procedure was managed as follows: applied substrates were precisely and sequentially cleaned with a surfactant, acetone, and isopropyl alcohol in an ultrasonic bath for 20 min in every solvent. The drying of the substrates took place on the ambient air, and additionally before deposition of the functional layers were treated by ultraviolet radiation for 15 min to remove all organic residues. Plasma-treated substrates were exposed to 10 s low-temperature ambient-air surfaceplasma generated by RPS40+ (Roplass s.r.o., Czech Republic). The surface of the uncleaned substrates was not treated in any way. First, a compact  $\text{TiO}_2$  sol-gel blocking layers prepared from the mixture of TiAcAc and  $\text{TiCl}_4$  precursors were spin-coated on the different pre-treated FTO substrates and sintered at  $500 \text{ }^\circ\text{C}$  for 30 min. Second, other functional layers of the C-PSC, such as mesoporous  $\text{TiO}_2$ ,  $\text{ZrO}_2$  and carbon back electrode were deposited by screen-printing. Third, the perovskite solution was directly dropped and infiltrated through the carbon layer and dried at  $100 \text{ }^\circ\text{C}$  for 30 min. A detailed method of C-PSC and  $\text{TiO}_2$  blocking layer preparation is described in the author's previous work [7].

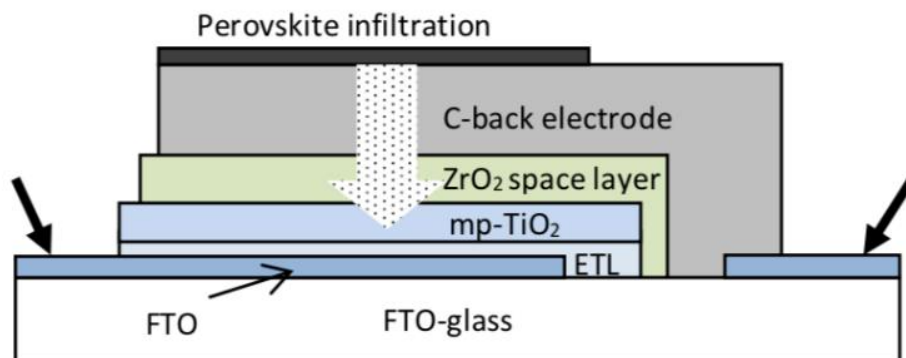


**Figure 1** The structure of the printed C-PSC

### 2.3. Characterisation

The conversion efficiency of solar to the electric energy of the C-PSC was determined by measuring photocurrent density-voltage load characteristics under  $1000 \text{ W/m}^2$  of standard daylight exposition with a 1.5G air-mass (AM). Optical microscope (*LEICA DM 2700 M*) and scanning electron microscope (*JEOL, JSM67500FA, Analytical field emission scanning electron microscope, Japan*) were used for the analysis of the FTO/ $\text{TiO}_2$  sol-gel surface. The X-ray photoelectron spectrometer Axis Supra from *Kratos Analytical* was used to study the surface chemistry of chemically cleaned, plasma-treated and uncleaned FTO samples.

### 3. RESULTS AND DISCUSSION

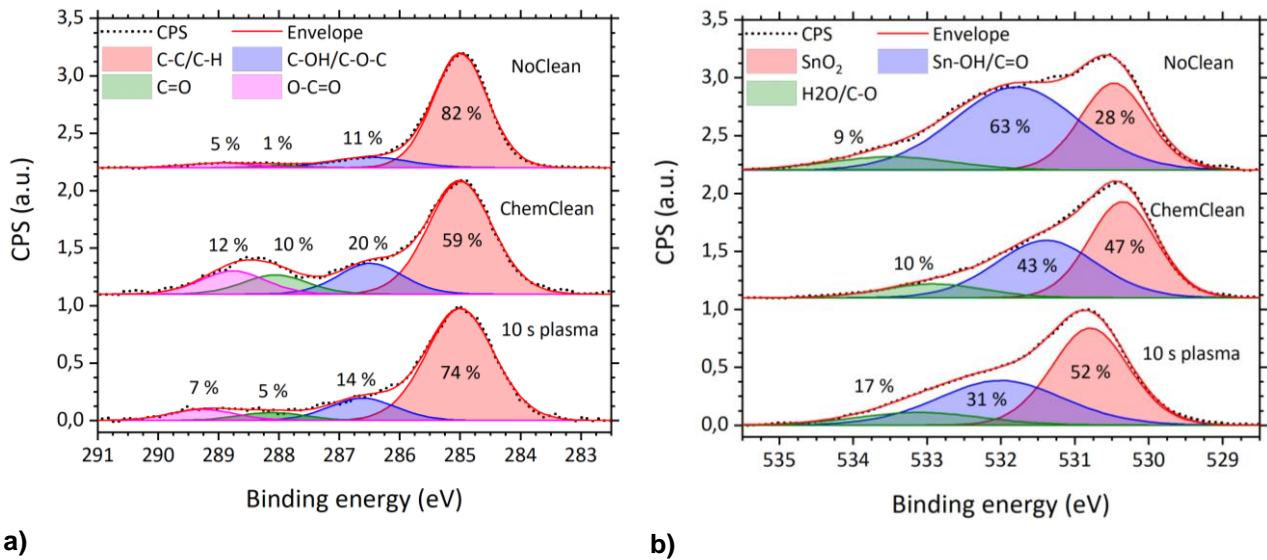
We analysed the reference, chemically cleaned and plasma-cleaned samples by X-ray photoelectron spectroscopy (XPS) to study the changes in the stoichiometry and bonding states on the surface of FTO glass. **Table 1** presents the elemental composition of the surface of FTO for different cleaning methods used. The uncleaned sample was highly contaminated, containing as much as 74% of carbon on the surface. Chemical cleaning process led to a decrease in carbon concentration on the surface to 26%. The uncleaned surface also contained traces (below 1%) of potassium and calcium, which were also reduced and in case of potassium completely removed after chemical cleaning. The oxygen concentration on the surface also increased, which can be attributed to the relative change in carbon concentration. Plasma cleaning of FTO for 10 s led to a decrease in carbon concentration to around 14%. The increase of oxygen on the surface was more significant compared to the chemical cleaning process. Exposure of the surface to the ambient air plasma, which contains reactive oxygen species causes oxidation of the surface and is known to induce polar oxygen-containing functional groups to the treated surface [8-10]. The O:C ratio (**Table 1**) therefore increased significantly. Compared to chemical cleaning, plasma treatment was not so efficient for the total removal of the potassium and calcium contamination. Around 4% of nitrogen was introduced to the surface of plasma-treated samples, a known effect of treatment by plasma generated in ambient air. These results correspond well with the plasma-cleaning of ITO with the same plasma source reported by *Homola et al.* [11].

**Table 1** Atomic concentrations from XPS with standard deviation measured at two points for each sample

	C [%]	O [%]	Sn [%]	Ca [%]	K [%]	N [%]	O:C	O:Sn
<b>No clean</b>	74 ± 7	19 ± 4	5 ± 3	0.7 ± 0.1	0.2 ± 0.0	1.0 ± 0.3	0.3	3.7
<b>Chem clean</b>	26 ± 1	49 ± 1	23 ± 1	0.3 ± 0.1	0.0 ± 0.1	2.1 ± 0.7	1.8	2.1
<b>10 s plasma</b>	14 ± 1	57 ± 0	23 ± 1	1.1 ± 0.3	0.8 ± 0.2	4.0 ± 1.0	4.0	2.5

The high-resolution C 1s region in the XPS spectrum is shown in **Figure 2a**. Four components were used for deconvolution, specifically C—C/C—H, C—OH/C—O—C, C=O and O—C=O species at 285.0 eV, 286.5 eV, 288.0 eV and 289.0 eV of binding energy, respectively. The reference sample without any cleaning displayed a significant C—C/C—H component with around 82% relative intensity. Chemical cleaning led to the removal of C—C/C—H groups from the surface, while the relative intensity of the oxygen-containing functional groups increased. The oxidation effect of the plasma can be seen in the increase of the relative intensity of the oxygen-containing functional groups in the C 1s region of the plasma-treated sample.

The high-resolution O 1s region is shown in **Figure 2b**. The SnO<sub>2</sub> in FTO typically displays a peak in the O 1s region at around 530.5 eV [12,13]. Furthermore, oxygen on metallic surfaces can be found in the form of metal-hydroxides (OH)<sup>-</sup>, that are often found in around 531.5 eV and in adsorbed H<sub>2</sub>O at around 533.0 eV [14,15]. Oxygen can also be found bound to carbon in a multitude of environments of the organic species, positions of which can vary between 531.0 eV up to 534.0 eV. We can expect significant contributions from the organic oxygen to the (OH)<sup>-</sup> and H<sub>2</sub>O components. Both chemical cleaning and plasma treatment led to a more pronounced SnO<sub>2</sub> component due to the removal of organic species. A shift of the SnO<sub>2</sub> component to higher binding energies can be seen after the plasma treatment. We believe that the surface of FTO prior to plasma treatment consisted of a mixture of Sn<sup>4+</sup> oxide and Sn<sup>2+</sup> oxide. Several author have shown that the signal in the XPS spectrum from the SnO is shifted from the signal from SnO<sub>2</sub> by around 0.4 eV towards lower binding energies [15-17]. The reactive oxygen species in plasma cause oxidation of the SnO into SnO<sub>2</sub> and therefore the shifted signal is observed.



a)

b)

**Figure 2** Comparison of narrow regions of **a)** C 1s and **b)** O 1s in the XPS spectrum of the uncleaned, chemically cleaned and plasma-cleaned surface of FTO

The photocurrent-voltage load characteristics of C-PSCs with all types of treated and uncleaned substrates are shown in **Figure 3**. It is evident, that the purity of the substrate's surface has a crucial effect on the quality of the deposited functional layers. Specifically on the blocking layers, as their thickness is several tens of nanometers and any impurity adversely affects all the photovoltaic parameters. The blocking layer with high quality without any cracks or failures prevents the recombination of electrons with holes, and also the internal short circuits what is necessary for high performance of C-PSC. Devices with substrates treated by the chemical way and by plasma for 10 s reached approximately the same efficiency 4.4 – 4.5% with relatively good shapes of photocurrent-voltage load characteristics, fill factor (FF) and short-circuit current density ( $J_{sc}$ ) (**Table 2**). The open-circuit voltage ( $V_{oc}$ ) has changed only partially from 0.65 to 0.70 V in all cases. Results achieved by the chemical cleaning can be attributed to a thin, homogeneous, and almost failure-free blocking layers, which was confirmed by optical and top-view SEM images (**Figures 4, 5a**). In the case of the substrates plasma-treated for 10 s, a small occurrence of impurities and defects in the blocking layers is seen in **Figures 4, 5b**. On the other hand, the effect of plasma improved the wettability of the FTO surface (contact angle decreased for plasma-treated FTO = 10° vs chemically cleaned FTO = 35°), and interfacial contact between the FTO and the blocking layer what led to better charge transport between the layers. The efficiency of C-PSCs with uncleaned substrates was at the level of 1% due to the presence of a large number of impurities, failures and pin-holes in the blocking layer (**Figures 4, 5c**). The presence of failures and pin-holes in the blocking layer created the trapping sites for charge recombination and current leakage what further led to a decrease in FF,  $J_{sc}$ , and to the linearisation of the load characteristics (**Table 2, Figure 3**). It can also be observed from optical images that the plasma, to some extent, cleans the surface of the substrate itself (**Figures 4b vs 4c**).

**Table 2** Photovoltaic parameters of the C-PSCs with differently treated and uncleaned substrates

Treatment	$J_{sc}$ (mA.cm <sup>-2</sup> )	$V_{oc}$ (V)	Efficiency (%)	FF
Uncleaned	8.4	0.70	1.4	0.23
Cleaned	15.8	0.68	4.4	0.41
Plasma 10 s	17.0	0.65	4.5	0.41

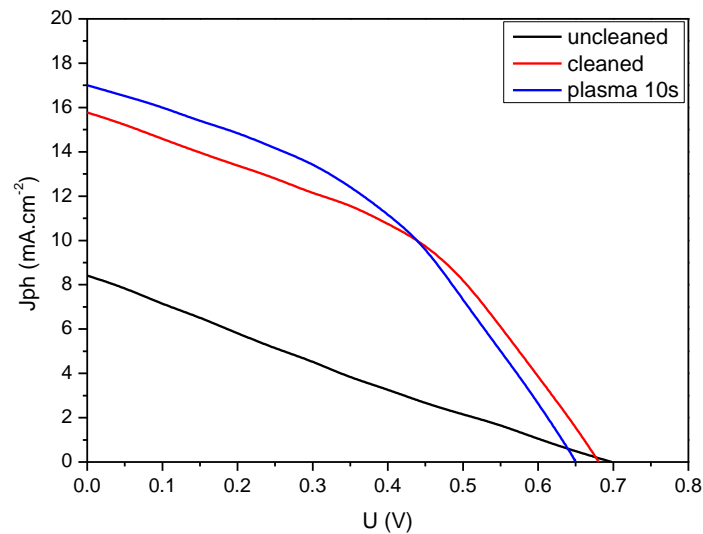


**Figure 3** J-V loading photo-curves of solar cells with differently cleaned and uncleaned substrates

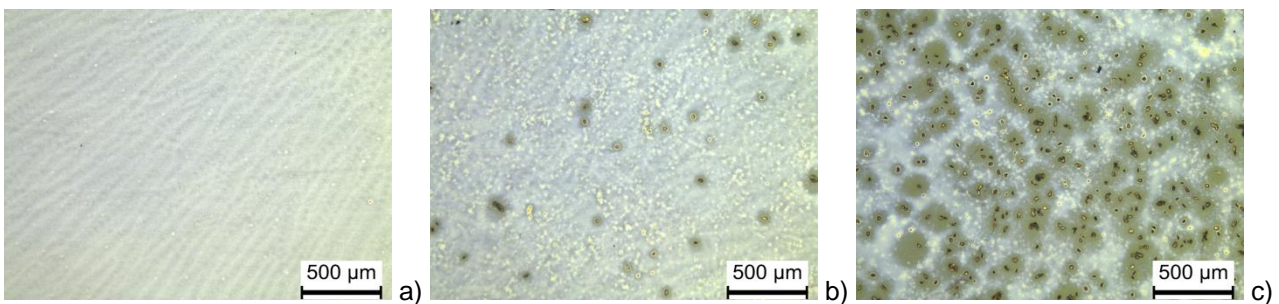


**Figure 4** Optical microscopy images of the TiO<sub>2</sub> sol-gel blocking layers prepared on: a) chemically cleaned substrate, b) 10 s plasma treated substrate and c) uncleaned substrate

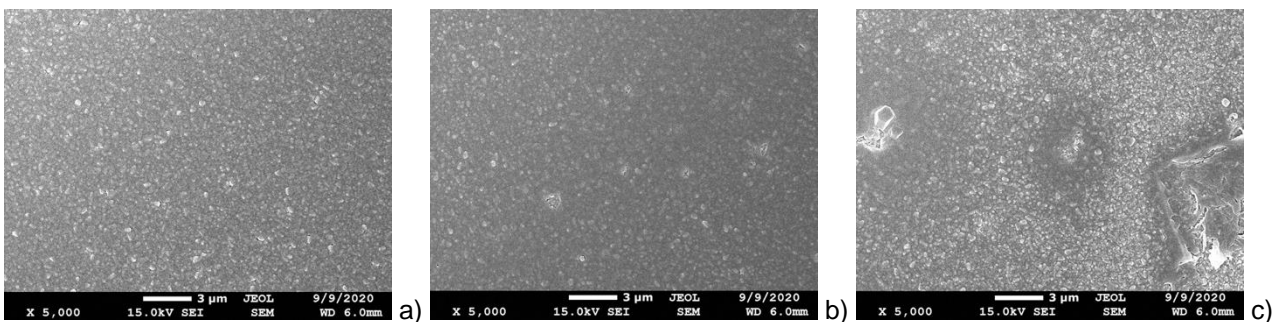


**Figure 5** Top-view SEM images (scale bar 3 μm) of the TiO<sub>2</sub> sol-gel blocking layers prepared on: a) chemically cleaned substrate, b) 10 s plasma-treated substrate and c) uncleaned substrate

#### 4. CONCLUSION

In this work, the mesoporous perovskite solar cells with carbon back electrode were prepared on chemically cleaned, plasma-treated and uncleaned substrates by screen-printing and coating technics. The obtained results showed that solar cells prepared on chemically cleaned substrates reached the approximately same efficiency and FF as on the substrates treated by 10 s low-temperature ambient air plasma. It means that the few second plasma treatments of FTO glass substrate can successfully replace protracted one hour chemically cleaning in different solvents and an ultrasonic bath.

## ACKNOWLEDGEMENTS

***This research was supported by the Slovak Grant Agency, VEGA 1/0488/19, STU Grant Scheme for Support of Young Researchers “PRINTCELL”, Czech Science Foundation project 19-14770Y and LM2018110 project funded by the Ministry of Education, Youth and Sports of the Czech Republic.***

## REFERENCES

- [1] MIKULA, M., BEKOVÁ, Z., HVOJNIK, M., HATALA, M., MIKOLÁŠEK, M., MULLEROVÁ, J., JERDEL, M., GEMEINER, P. Differently sintered TiO<sub>x</sub> hole blocking layers for solution processed solar cells. *Applied Surface Science*. 2018, no. 461, pp. 54-60.
- [2] LIU, H., FU, X., BALA, H., ZONG, B., HUANG, L., FU, W., WANG, S., GUO, Z., SUN, G., CAO, J., ZHANG, Z. An effective TiO<sub>2</sub> blocking layer for hole-conductor-free perovskite solar cells based on carbon counter electrode. *Organic Electronics*. [online]. 2018. Available from: <https://doi.org/10.1016/j.orgel.2018.04.042>.
- [3] LIAN, J., LU, B., NIU, F., ZENG, P., ZHAN, X. Electron-Transport Materials in Perovskite Solar Cells. *Small Methods*. 2018, Vol. 2, 1800082.
- [4] MOHAMAD NOH, M.F., TEH, C.H., DAIK, R., LIM, E.L., YAP, C.C., IBRAHIM, M.A.A., AHMAD LUDIN, N., MOHD YUSOFF, A.R.B., JANG, J., MAT TERIDI, M.A. The architecture of the electron transport layer for a perovskite solar cell. *Journal of Materials Chemistry C*. 2018, vol. 6, pp. 682-712.
- [5] FAGIOLARI, L., BELLA, F. Carbon-based materials for stable, cheaper and large-scale processable perovskite solar cells. *Energy and Environmental Science*. 2019, vol. 12, pp. 3437-3472.
- [6] HOMOLA, T., SHEKARGOFTAR, M., POSPÍŠIL, J. Atmospheric plasma treatment of ITO thin films for rapid manufacturing of perovskite solar cells. In: *11th International Conference on Nanomaterials - Research & Application*. [online]. Brno:Tanger, 2019, pp. 43-47. Available from: <https://doi.org/10.37904/nanocon.2019.8645>.
- [7] HVOJNIK, M., POPOVIČOVÁ, A.M., PAVLIČKOVÁ, M., HATALA, M., GEMEINER, P., MÜLLEROVÁ, J., TOMANOVÁ, K., MIKULA, M. Solution-processed TiO<sub>2</sub> blocking layers in printed carbon-based perovskite solar cells. *Applied Surface Science*. 2020, vol. 536, 147888.
- [8] VESEL, A., MOZETIC, M. New developments in surface functionalization of polymers using controlled plasma treatments. *J. Phys. D. Appl. Phys.* [online]. 2017, vol. 50, no. 29. Available from: <https://doi.org/10.1088/1361-6463/aa748a>.
- [9] KHOMIAKOVA, N., HANUŠ, J., KUZMINOVA, A., KYLIÁN, O. Investigation of Wettability, Drying and Water Condensation on Polyimide (Kapton) Films Treated by Atmospheric Pressure Air Dielectric Barrier Discharge. *Coatings*. 2020, vol. 10, no. 7, p. 619.
- [10] KUZMINOVA, A., VANDROVCOVÁ, M., SHELEMIN, A., KYLIÁN, O., CHOUKOUROV, A., HANUŠ, J., BAČÁKOVÁ, L., SLAVINSKÁ, D., BIEDERMAN, H. Treatment of poly(ethylene terephthalate) foils by atmospheric pressure air dielectric barrier discharge and its influence on cell growth. *Applied Surface Science*. 2015, vol. 357, part A, pp. 689-695.
- [11] HOMOLA, T., MATOUŠEK, J., MEDVECKÁ, V., ZAHORANOVÁ, A., KORMUNDA, M., KOVÁČIK, D., ČERNÁK, M. *Appl. Surf. Sci.* [online] 2012, vol. 258, no. 18, pp. 7135–7139. Available from: <https://doi.org/10.1016/j.apsusc.2012.03.188>.
- [12] SWALLOW, J.E.N., WILLIAMSON, B.A.D., WHITTLES, T.J., BIRKETT, M., FEATHERSTONE, T.J., PENG, N., ABBOTT, A., FARNWORTH, M., CHEETHAM, K.J., WARREN, P., et al. Self-Compensation in Transparent Conducting F-Doped SnO<sub>2</sub>. *Advanced Functional Materials*. [online]. 2017, vol. 28. Available from: <https://doi.org/10.1002/adfm.201701900>.
- [13] MARTÍNEZ, A.I., HUERTA, L., O-RUEDA DE LEÓN, J.M., ACOSTA, D., MALIK, O., AGUILAR, M. Physicochemical characteristics of fluorine doped tin oxide films. *J. Phys. D. Appl. Phys.* [online]. 2006, vol. 39, no. 23, pp. 5091-5096. Available from: <https://doi.org/10.1088/0022-3727/39/23/029>.
- [14] JADHAV, H., SURYAWANSHI, S., MORE, M.A., SINHA, S. Pulsed laser deposition of tin oxide thin films for field emission studies. *Appl. Surf. Sci.* [online]. 2017, vol. 419, pp. 764-769. Available from: <https://doi.org/10.1016/j.apsusc.2017.05.020>.

- [15] GAGGIOTTI, G., GALDIKAS, A., KAČIULIS, S., MATTOGNO, G., ŠETKUS, A. Surface chemistry of tin oxide based gas sensors. *J. Appl. Phys.* [online]. 1994, vol. 76, no. 8, pp. 4467-4471. Available from: <https://doi.org/10.1063/1.357277>.
- [16] SZUBER, J., CZEMPIK, G., LARCIPRETE, R., KOZIEJ, D., ADAMOWICZ, B. XPS study of the L-CVD deposited SnO<sub>2</sub> thin films exposed to oxygen and hydrogen. In: *Thin Solid Films*. [online]. Vol. 391, pp. 198-203. Available from: [https://doi.org/10.1016/S0040-6090\(01\)00982-8](https://doi.org/10.1016/S0040-6090(01)00982-8)
- [17] LIANG, L.Y., LIU, Z.M., CAO, H.T., PAN, X.Q. Microstructural, Optical, and Electrical Properties of SnO Thin Films Prepared on Quartz via a Two-Step Method. *ACS Appl. Mater. Interfaces*. [online]. 2010, vol. 2, no. 4, pp. 1060-1065. Available from: <https://doi.org/10.1021/am900838z>.